CALCULATION OF DESIGN LOADS FOR THE MOD-5A 7.3 MW WIND TURBINE SYSTEM

L. Mirandy, General Electric Co.
J. C. Strain, General Electric Co.

ABSTRACT

Design loads are presented for the General Electric MOD-5A wind turbine. The MOD-5A system consists of a 400 ft. diameter, upwind, two-bladed, teetered rotor connected to a 7.3 MW variable-speed generator. Fatigue loads are specified in the form of histograms for the 30 year life of the machine, while limit (or maximum) loads have been derived from transient dynamic analysis at critical operating conditions. Loads prediction was accomplished using state of the art aeroelastic analyses developed at General Electric. Features of the primary predictive tool - the Transient Rotor Analysis Code (TRAC) are described in the paper. Key to the load predictions are the following wind models: (1) yearly mean wind distribution, (2) mean wind variations during operation, (3) number of start/shutdown cycles, (4) spatially large gusts, and (5) spatially small gusts (local turbulence). The methods used to develop statistical distributions from load calculations represent an extension of procedures used in past wind programs and is believed to be a significant contribution to Wind Turbine Generator analysis. Test/theory correlations are presented to demonstrate code load predictive capability and to support the wind models used in the analysis. In addition, MOD-5A loads are compared with those of existing machines.

The MOD-5A design was performed by the General Electric Company, Advanced Energy Program Department under Contract DEN3-153 with NASA Lewis Research Center and sponsored by the Department of Energy.

INTRODUCTION

The MOD-5A was designed by the General Electric Company as part of the Department of Energy sponsored program to develop multi-megawatt, utility-class, wind turbine generators. It is a two-bladed, horizontal-axis, 400 foot diameter, upwind design. The MOD-5A features a teetering rotor and laminated wood blades with ailerons over the outboard 40% of the blades to regulate power and to shut down. It incorporates a 7.3 megawatt variable- speed generator. However, to avoid resonances, there are only two nominal rotor speeds - 13.8 and 16.8 RPM. Additional aspects and further discussion of the MOD-5A are contained in Reference 1.

This paper summarizes the loads analysis conducted for the MOD-5A. The analytical techniques are described, followed by comparison of theoretical predictions with test data to support the methods and models used. Test data were taken from the General Electric 2MW, 200 ft. diameter MOD-1, the Boeing 2.5MW, 300 ft. diameter MOD-2, and the Hamilton Standard 4MW, 256 ft. diameter SVU-WTS 4. The MOD-5A design loads presented, herein, are 15% to 25% higher than the theoretical predictions to allow for uncertainties. The machine has been designed to these loads.

METHODS OF ANALYSIS

The WTG loads analysis began with the construction of a dynamic model to determine the natural modes and frequencies of the system. State-of-the art finite element and modal-synthesis techniques were applied. Since these methods are accepted standards in the aerospace industry, they will not be addressed here. Rather, we will focus on the aeroelastic and wind models used for the wind turbine loads analysis.

The experience gained, and methods developed during the MOD-1 program served as a cornerstone for the MOD-5A analysis. Extensive correlation studies and code verification exercises were conducted before the MOD-5A program. Our loads prediction

capabilities were enhanced during the MOD-5A program, particularly in the areas of transient analysis, wind modelling and load statistics. These topics are discussed in the following paragraphs.

Aeroelastic Codes

Two aeroelastic codes were used to predict design loads for the MOD-5A: GETSS, General Electric Turbine System Synthesis and TRAC, Transient Rotor Analysis Code.

GETSS - GETSS was developed during the MOD-1 program and was used to predict the MOD-5A's fatigue loads during the preliminary design phase. The code was verified by NASA during the MOD-1 program, by correlating its predictions with MOD-0 test data. It provided excellent load estimates for MOD-1 and was verified for soft tower and teetering rotor configurations during the MOD-5A contract.

The GETSS analysis flow is shown in Figure 1. The system's structural dynamics are approximated by piecewise linear models of the entire system; wherein natural modes are input for discrete rotor positions. As the blades rotate, the dynamical equations switch from one model to the next. A time history solution is determined over as many revolutions as are required to produce a steady-state response; the last rotor cycle is then used to compute steady-state fatigue loads. Aerodynamic and gravitational forces are computed as a function of the rotor position by the computer code, WINDLD, before the time history calculations, and are applied to the right side of the modal equations. Aeroelastic coupling comes from aerodynamic modal damping coefficient calculations computed by the computer code, QAERO, before the time history calculations. Finally, interface design loads are computed from the modal response. The code can handle a large number of system modes at relatively low computational cost, because the modal equations are decoupled linear, second-order equations, for which there are very efficient numerical integration algorithms. More detailed code descriptions may be found in the MOD-1 final design report (Ref. 2).

TRAC - TRAC was developed during the MOD-5A program to predict transient loads.The program was checked, using steady-state loads calculated by the GETSS code as a benchmark. The verification provided confidence in the calculations made by both programs. In this paper, we show correlation between TRAC fatigue and limit load predictions with MOD-1 data. TRAC also agreed qualitatively with MOD-2 on the subject of interactions between the structure and the control system. TRAC was used to compute all the MOD-5A's final design loads.

The self-explanatory features of the code are illustrated in Figure 2. It does not use piecewise-linear modal inputs, as GETSS does. Rather, separate inputs are provided for rotating and fixed system modes. Complete inertial and aerodynamic coupling between the degrees of freedom has been retained in the development. Furthermore, non-linear inertia terms, caused by finite elastic deflections of the blade, are included. As such, the equations are highly coupled. A Runge-Kutta numerical integration has been used to obtain solutions. Loads are calculated after each time step using the "modal acceleration" technique, which is superior to basing loads on elastic deflections (modal deflection technique). When the rotor speed varies during a transient solution, the blade stiffness terms are adjusted using Southwell coefficients, which are computed within the program. The NASA interim turbulence model was incorporated into the code for fatigue load computation, however, the capability of analyzing only wind shear or tower shadow, or both, was retained.

Wind Models

The wind models used to compute design loads are classified in Table 1. Wind models used for limit and fatigue load calculations appear separately. The same large gust model is used in each case (I.2 and II.3). Models II.2, II.3, and II.4 will be described in this section. The other models appearing in the table are self-explanatory.

MEAN WIND VARIATIONS - These variations produce shifts in mean load levels which must be considered as fatigue cycles. For example, if the machine is

operating in a 20 mph wind and during 10 minutes the wind shifts to 30 mph and returns to 20 mph, a fatigue cycle results from the difference in load levels at 20 and 30 mph. The load shift, which can be viewed as a "DC" phenomenon, was dubbed a Type IIA load. In order to quantify the variation in mean wind speed, 4 months of data taken at Amarillo, TX by PNL-Battelle was statistically analyzed. Figure 3 outlines the analysis and the results. In addition to mean wind shift statistics, the data was used to compute the number of start-stop cycles that would be experienced by a MOD-5A. It might be added that the yearly wind speed distribution at Amarillo is quite similar to the specification tn the MOD-5A Statement of Work.

LARGE GUSTS - Figure 4 summarizes the large gust model used for the MOD-5A design. The MOD-5A Statement of Work wind PSD specification was integrated to determine the root mean square gust value. The cut-off frequency of .02 Hz, used in the integration, was based on a spatial coherence model developed during MOD-2, and used in conjunction with the MOD-5A rotor diameter. The relevant formula appears below:

$$COH = \exp-(fxdK_V)$$

where:

- f = cut-off frequency (Hz)
- x = fraction of rotor disc for which the coherence is sought. A value of 1.0 (or the whole disc) was used.
- d = rotor diameter (meters)
- K_V = .37 - .005V, V = wind speed (m/s)

Gusts having a coherence equal to or greater than 0.50 were conservatively treated as rotor encompassing gusts. This formula leads to a cut-off frequency of .018 Hz at 25 mph and .022 Hz at 50 mph. An average of .02 Hz was used for all wind speeds. This cut-off frequency implies an average gust period of 50 seconds, which is supported by MOD-2 test measurements discussed in the verifcation section of this paper. A Rayleigh distribution was selected for the gust amplitudes on the basis of PNL-Battelle's "Gust-O" measurements reported in PNL 3138. The gust model in Figure 4 is used to compute both fatigue loads and limit loads. It will be shown that MOD-2 loads data supports the gust amplitudes we have used.

LOCAL TURBULENCE - Gusts smaller than the rotor diameter produce variations in the apparent wind speed experienced by the rotating blades at harmonics of the rotor speed. The situation is illustrated in Figure 5. This harmonic forcing produces fatigue loads which occur every rotor cycle. Measurements and data analysis conducted by PNL-Battelle identified and began to quantify the magnitudes of these turbulent inputs. NASA developed an "Interim Turbulence Model" from this data, which conveniently expresses the root mean square values of the harmonic forcing for rotors of different sizes. GE adopted NASA's model and extended it to include gust probabilities. The formulas are summarized in Table 2. GE assumed the probability distribution of the random harmonic coefficients was Rayleigh, as would be the case for a narrow-band process. The Rayleigh assumption also seems to be supported by the ratios of 99.9th percentile to 50th percentile loads generally found in flap bending moment test data. Correlation of this turbulence model with MOD-1 loads appears in the verification section of this paper.

Load Statistics

Fatigue loads for the MOD-5A were expressed as probability distributions (or histograms) to be applied for the 30-year life of the machine. This section describes the methodology used in deriving the fatigue load statistics. Fatigue loads were segregated into three categories, shown in Figure 6; the same categories used in previous wind turbine generator programs. The Type I loads represent the alternating loads, which occur at 1 or 2P (where P stands for "per revolution"). For design purposes, all load components were conservatively assigned a 2P occurrence rate. The local turbulence model was used to derive Type I loads. The Type II loads stem from gusts, that cause a shift in mean load during the gust. This mean shift, and the normally occurring alternating loads were used to compute a cycle of fatigue loading for each gust occurrence. The large gust model was used to compute Type II loads. Similar Type IIA loads, which stem from longer mean wind speed variations, are not shown in the figure. The Type III loads represent the "ground to air to ground" cycle and have a frequency

of occurrence equal to the number of start-stop cycles. Type III loads were computed from the delta loads between normal operation, through shutdown, to the parked state. Note that shutdown transients can produce wider deltas in some load components than simply considering the normal operating and parked conditions. The number of Type I, II, IIA, and III cycles expected over 30 years are 3.5×10^8, 1.4×10^7, 1.5×10^6 and 35,000, respectively.

The first step in determining the life cycle fatigue loads was to obtain the mean wind statistics of the site. The wind specification in the Statement of Work was used for MOD-5A. The operation of the wind turbine was separated into discrete wind bins, as illustrated in Figure 7. The total number of Type I cycles, which was based on the number of rotor cycles, and Type II cycles, which was based on the number of gusts, were computed for each bin.

In the second step, mean and alternating steady-state loads were computed from cut-in to cut-out speeds, using TRAC. The wind speeds analyzed did not necessarily correspond to the bin mean wind speeds; instead a sufficient number of wind speeds was chosen to construct smooth curves of load versus wind velocity. In this way, the data could be applied to wind sites other than the one selected. The steady-state loads were computed using the root mean square wind speed harmonic variations given by the NASA Interim Turbulence Model. The third step determined the distribution of Type I loads for each bin. First the steady-state loads data were converted to 50th percentile values on the basis of a Rayleigh distribution. Data measurements from existing wind turbines indicated that Type I loads were well fitted by a log-normal distribution and so this distribution was used to compute loads at other percentiles. The slope of the distribution was based on existing teetered rotor test data. It is believed that the log-normal distribution stems from the sum of a constant (or deterministic) load level and stochastic loads with a Rayleigh distribution. This premise was supported by the MOD-1 fatigue load correlation study reported in the subsequent section, wherein loads were computed for various turbulence amplitude percentiles and were compared to measured values. Both the measurements and predictions appearred to be log-normal.

In the fourth step, of Figure 7, the procedures used to obtain Type II and Type IIA loads are summarized. A probability distribution of gust amplitude was constructed on the basis of the wind turbulence model. Mean and alternating loads were used to determine the Type II loads corresponding to a sufficient number of discrete gust amplitudes. The load probabilities were equal to the gust probabilities from which they were derived. The zeroth percentile load (no gust) was equal to the steady-state, 50th percentile load. Note that the Type II load distribution was not assumed to follow any prescribed probability law; instead it was constructed directly from the wind turbulence model and associated response load. Type II calculations were further refined to account for load amplification during a gust, which is caused by the dynamics of the control system.

Type III loads were determined from the differential load encountered in the transition between normal operation and the parked state.

Finally, in the sixth step, composite fatigue histograms were constructed from all the data. These histograms define the total fatigue loading that is projected to occur over 30 years. The cyclic loads are presented in the form of a histogram as shown, or equivalently as a cumulative probability. These loads, along with statistics of the corresponding mean loads, were supplied to the designers. The procedure was computerized, for rapid turnaround and to allow life cycle loading for various wind sites to be generated with little effort.

VERIFICATION OF CODES AND MODELS

The GETSS code was correlated with MOD-0 data supplied by NASA during the MOD-1 program and during the conceptual design of the MOD-5A. These validation results will not be repeated here. Rather, this section focuses on substantiating the wind models that have been adopted and the loads predicted by the TRAC code. Specifically, it will cover shutdown transients, Type I load probability

distributions and Type II loads in the subsequent paragraphs.

Shutdown testing performed during the MOD-1 check-out was simulated using the TRAC code. Figure 8 shows a typical simulation, in which rotor speed, pitch angle, and blade flap bending moment at .35R are plotted versus time. Following about 3 seconds of steady-state operation at 25 rpm, the blades were feathered at 8°/sec for 1.5 seconds followed by a 2°/sec pitch rate for the remainder of the shutdown. (The dual feather rate was used on MOD-1 to guard against high loads). The time histories show that the rotor speed decreased continuously after feather, while the flap bending moment reached a peak at about 5 seconds. Similar analyses were conducted for shutdowns from other initial rotor speeds and the peak flap bending loads were recorded. Figure 9 compares theoretically predicted loads with test measurements made at two blade stations. Here, peak moments were plotted against the rotor speed at which the shutdown was initiated. There was excellent agreement between the test and the theory.

Probability distributions of MOD-1 flap-bending moments measured at three blade radial stations are compared with theoretical predictions in Figure 10. These represent Type I cyclic (1/2 peak-peak) loads. A band of measured data is shown along with discrete test points taken on a typical day of operation. The theoretical loads were computed using NASA's Interim Turbulence Model with the TRAC code. Points at three percentiles were generated by ascribing turbulence disturbance amplitudes according to a Rayleigh distribution. Tower shadow was also included in the model. The results indicated excellent agreement between test and theory at mid-span, while predictions were at the top and bottom of test scatter for outboard and inboard locations, respectively. In view of the contingency factors of 15-25%, which were applied to all MOD-5A load predictions, the turbulence model was considered to be satisfactory for design purposes.

Type II loads were extracted from MOD-2 data tapes supplied by NASA. Occurrances were counted according to positive slope crossings of the mean load versus time. Figure 3 shows the similar procedure, used for wind data. Figure 11 contains a table of the frequency of Type II load occurrances along with the number of wind speed shifts. Note that there are more cycles of the wind speed point measurement (81.9/hr.) than of the loads (55-61/hr.), which makes sense because all the shifts in wind speed may not be spatially large enough to cause a change in mean rotor loads. Below the table, a scattergram of Type II load magnitude is plotted against load period. Higher loads correspond to higher periods, as would be expected because the large rotor enveloping gusts have longer periods. About a 50 second period, or more, was needed to produce peak load levels. The average frequency of MOD-2 loads (55-61/hr.) agreed well with what was modelled for the MOD-5A (65/hr.). If anything, the MOD-5A would be expected to have a lower frequency because of its increased size, so this analysis was slightly conservative.

Type II load probability distributions are plotted in Figure 12. MOD-5A predictions for similar wind conditions are also shown. The MOD-5A predictions were in line with the scaled test data, if not somewhat conservative. This analysis provided confidence in the modelling of Type II loads on the MOD-5A.

MOD-5A DESIGN LOADS

System Dynamic Model

The natural modes and frequencies were calculated from a model of the MOD-5A system. The dynamic mathematical model was made up of models of each substructure, which were unified by the stiffness coupling method of modal synthesis. The MOD-5A wind turbine substructures and their coupling interfaces are shown in Figure 13. The substructures were the rotor, the yoke and rotor support, the bedplate and nacelle and their associated hardware, and the tower.

The natural modes and frequencies of each substructure, except the blade, were calculated using NASTRAN or a similar finite element program. The blade modes and frequencies were determined using a proprietary GE program called STRAP (Static Row Analysis Program). STRAP is a finite element

beam modelling program that includes the stiffening effects of centrifugal forces.

The stiffness links used to unify the substructures were derived as follows:

- Rotor to Yoke - The links were derived from stiffness data obtained from the manufacturer of the teeter bearing. The teeter bearing is elastomeric and has stiffness in all 6 degrees of freedom.
- Low Speed Shaft to Bedplate - The links were calculated by inverting a bedplate flexibility matrix obtained from detailed NASTRAN load cases.
- Bedplate to Tower - The link was derived from manufacturer's data on the yaw bearing and yaw hydraulics, and from the structural design of the upper yaw housing (the lower yaw housing was included in the tower finite element model). A scaler spring element was created from yaw bearing stiffnesses in 5 degrees of freedom and yaw brake stiffness (or yaw hydraulic stiffness depending on the case investigated) in the yaw degree of freedom. This scalar spring was then added in series with a beam model of the upper yaw housing.

SCAMP (Stiffness Coupling Approach Modal-synthesis Program), a proprietary GE computer program, unified the substructures. This modal synthesis method has been used extensively at the General Electric Space Division for spacecraft analysis and was also successfully used in the MOD-1 program. The method uses the free substructure vibration modes and frequencies to determine the modes of the entire system. These substructures, as defined by the stiffness coupling method, have no common degrees of freedom and are coupled together by the stiffness links that relate the free attachment coordinates of the substructures. Details of the method are documented in Reference 3.

The system modes and frequencies were calculated with the blades in both the vertical and horizontal positions. Typical mode shapes with the rotor in a vertical position are shown in Figure 14. The drive train and teetering modes are simply rigid body rotations of the rotor about the drive shaft and teeter pin, with little or no motion of the remaining system elements. The fundamental tower bending mode, shown for the direction normal to the axis of rotation, exhibits a small amount of yaw rotation caused by the offset center of gravity of the nacelle. The tower bending mode in the direction of the drive shaft axis is not shown, but it has nearly the same natural frequency, and considerably more blade elastic deflection in the softer flapwise direction. The final elastic mode shape displays collective flapwise bending of the blades. The mode shape plots are used to provide insight into the response of the system.

Table 3 contains a summary of the system natural frequencies for the baseline design. The calculations were made with the blades in vertical and horizontal positions at 13.8 and 16.8 rpm. Frequencies are shown in Hz and P. The numbers in parentheses denote P values at the 13.8 rpm. The last column earmarks the harmonics that should be avoided in each mode. E stands for even, and O, for odd. For example, fixed system modes of the tower must avoid even integers of rotor speed with a two bladed rotor, while rotor cyclic modes must avoid odd integers. Figure 15 depicts frequency placement of the MOD-5A graphically. The hatched areas indicate frequency ranges that should be avoided, to preclude resonant excitation. Symbols connected by horizontal lines indicate that the frequency changes in going from a vertical to horizontal blade position.

All system frequencies are well placed with the possible exception of the first flap collective which is at 4.2P. The blade design, however, is compatible with the loads predicted for this blade. Furthermore, dominant blade fatigue stresses were due to chord bending loads which are not effected by this frequency. There is still reason for concern, though, because of the uncertainty in some variables used in the load calculations. The variable most in question is the amount of 4P turbulence in the wind at the chosen site. The loads would be sensitive to this turbulence, since the blade resonance is near the excitation frequency. To eliminate this risk, methods to raise or lower the flapwise frequency were investigated near the end of final design. Three feasible avenues were identified:

1. Structural modification - (blade thickness and/or chord).
2. Addition of ballast weight to the outboard blade (the earlier, heavier,

partial-span-control configuration had a desirable 3P frequency, which increased to the present 4.2P when lighter weight ailerons were substituted in their place).

3. Change of operating RPM (this could be done in the field on the MOD-5A because of the variable-speed-gnerator).

Were the MOD-5A to be built, it is likely that one of the above modifications would be implemented to minimize risk.

Design Operating Conditions

The MOD-5A loads were based on cut-in and cut-out wind speeds of 14 mph and 60 mph, respectively, at the hub height . Fatigue cycles for 30 years of operation were computed for the MOD-5A Statement of Work Wind Duration Curve. The wind bins used to generate the fatigue data are summarized in Table 4, along with the numbers of Type I, II, and IIA cycles for each bin. Gust and mean wind shift amplitudes at the bin mean wind speeds are contained in Table 5. Gust amplitudes up to and including the 99.9th percentile were used to predict the fatigue loads. The 99.99th percentile gust was used to compute limit loads.

Critical operating conditions used to compute limit loads are summarized in Table 6. The system was designed to withstand the first four conditions without damage. The last case represented an extreme condition, which the MOD-5A could withstand without catastrophic failure such as losing a blade. Table 7 summarizes additional events which were analyzed, but were not critically important for the MOD-5A.

Interfaces Loads

The design loads were calculated at the locations listed in Table 8. A full set of shear and moment loads (V_x, V_y, V_z, M_x, M_y, M_z) were supplied at these points. The sign conventions for the main blade and the fixed system are shown in Figure 16. The coordinate directions lie on principal axes and twist with the cross-sections of the blade airfoil. The dimensions of the system and the locations of the non-blade interfaces are shown in Figure 17.

The interface design loads were specified in 3 sets of tables:

(1) histograms combining Type I, Type II, and Type IIA fatigue loads (359×10^6 cycles in 30 years)

(2) Type III fatigue loads (35,000 cycles in 30 years)

(3) limit loads for each critical operating condition

Because of the volume of this data, only highlights are presented herein.

A sample histogram is displayed in Table 9. Each row corresponds to a bar of the histogram. Columns 1 and 2 provide the number of cycles in and the cumulative probability associated with each bar. The range of cyclic loads for each bar, the bar width, is defined in columns 3 and 4. Columns 5 and 6 are these same dimensional loads divided by the maximum cyclic value, while columns 7 and 8 are similarly non-dimensionalized by the 50th percentile cyclic load at the rated wind speed. The remaining columns provide statistics of the mean, or mid-range, load for each bar of the histogram. Included below the table are the root-mean-cubed value of all cyclic load occurrences and the average mean load for 30 years of operation.

Probability distributions of alternating blade flap bending moments are shown in Figure 18 for three radial stations. The load magnitudes have been divided by the mean flap-bending moment at the rated wind speed, 32 mph, to allow comparison with data from other wind turbines. The curves display a slight increase in slope above the 99.9th percentile that is caused by Type II load occurrences. Type III fatigue levels, indicated by horizontal lines, are slightly greater than the maximum Type I and II values. To lend credence to the predictions, scaled test data from the Boeing MOD-2 and Hamilton Standard SVU2 wind turbines are included on the plot. This data suggests that MOD-5A predictions are appropriate, and even somewhat conservative. Figure 19 contains probability distributions of the alternating blade chord bending moment, normalized by the one-g moments. Here the loads are dominated by gravity, so there is only a slight increase between the 50th and 99.99th percentile. This trend was also true for MOD-2 test results, which are not shown.

Tower fatigue bending moment distributions are plotted in Figure 20. In this case the alternating moments at the base of the tower have been normalized by the mean bending moment created by the rotor aerodynamic thrust at rated wind speed. The alternating thrust moment (My) is far more sensitive to gusts than Mz, which accounts for the differences in the probability distributions. The MOD-5A predictions appear to be consistent with MOD-2 data, which is also included in the figure. The earlier MOD-2 data, in the upper curve, was taken before improvements were made to the control system, so it exhibits higher loads.

Vibratory rotor torques are plotted in Figure 21. Alternating torque levels, and likewise power levels, are below 10% of rated torque for over 90% of the operating time. The pronounced increase in load above the 98th percentile is due to Type II gusts and shifts in mean wind speed. Curves of yaw bearing moments and drive torque are included in Figure 22.

Normalized blade limit loads are summarized in Figure 23. The flap bending moments are from 2.25-3 times the mean moment at rated wind speed. Chord bending moments are about 2 g's at the root, where gravitional effects are greatest. They increase to about 9 g's at the tip, where the aileron drag forces far exceed the one g loads. Normalized fixed system limit loads are reported at selected interfaces in Table 10.

Selected Component Loads

Ailerons

The coordinate system used to define loads on the aileron is illustrated in Figure 24. Again, the axes are fixed to the structure and rotate with the aileron. Unlike other load components, local aileron loads are defined by running shears (V_x, V_y, V_z in lb/ft) and a running hinge moment (M_h in ft-lb/ft) as a function of the blade span, from the start of the aileron at .60R to the outmost section at .99R. Load/unit span rather than stress resultants were used, because this allowed the hinge locations and their end conditions to be varied during the design without changing the external loads. Furthermore, aerodynamic and inertial loads are specified separately, so that the inertia loads could be made consistent with the actual final design weight by using appropriate g factors.

Operational limit loads appear in Figures 25 and 26. The airloads were based on an aileron deflection of -45°, which is greater than would be needed to stop the machine. Thus, these loads are somewhat greater than would be experienced with the MOD-5A, which has force-limited actuators to prevent excessive aileron angles during critical conditions. In addition to the overspeed-shutdown, the ailerons were also designed to withstand a 130 mph hurricane wind while parked. With the exception of inboard pitching moments, the hurricane condition is less critical.

Fatigue loads have been defined by mean and alternating load components. The aerodynamic mean loads are shown in Figure 27. These loads were applied for all fatigue cycles, while the alternating loads noted in the figure caption were assigned probability distributions similar to the main blade. Alternating inertia loads (not shown) are on the order of one g, while the dominant steady load is due to centrifugal force.

Because the design for the ailerons was not as mature as other system components, these structural loads were developed conservatively. This approach was adopted to ensure a safe configuration on the first design iteration.

Blades

Stress resultants acting on the main blade structure were defined at the interfaces quoted in Table 8. These loads, which were discussed earlier, were used to size the primary structure of the blade. In this section, blade internal and external pressure distributions are addressed. These produce membrane and plate bending stresses.

The pressure loads on the blade are closely related to blade venting, because venting influences the internal pressure. A blade sealed against the atmosphere would experience excessive pressure loads. Therefore, a vented design was adopted. Inboard and outboard vents were incorporated, because they minimize pressure loads and promote a

sanitary environment inside the blade. The trailing edge section, which extends from the blade root to the ailerons at .60R, is vented at .10R and .60R. The two forward cells of the blade cross-section are vented at .10R and the tip (1.0R).

The internal pressure in the cavities of the blade at the non-dimensional spanwise station, x, is given by:

$$p_g = p_i - p_o = q_t \left(x^2 - \frac{1}{2}\left(x^2_1 + x^2_2\right)\right)$$

where,

$$q_t = \frac{1}{2} \rho V^2_t$$

ρ = air density

V_t = tip speed

x_1 and x_2 are the non-dimensional spanwise locations of the vents

p_i = absolute pressure in the cavity at station x

p_o = vent pressure (taken to be atmospheric)

p_g = gage pressure within the cavity

The external pressures on the blade surface are obtained from the airfoil pressure distribution. Figure 28 contains plots of airfoil pressure coefficient (Cp) vs the chordwise location for critical operating conditions. This data is furnished at three spanwise locations, x = .25, .55, and .95. Dimensional gage pressures on the exterior surfaces are given by

$$p_g = p_e - p_o = q_t x^2 C_p$$

The external pressures were used with the previously defined internal pressures in the blade structural analysis. The following pressures for the parked blade in hurricane conditions were also analyzed:

internal gage pressure = 0

external gage pressure = $1/2\ \rho V^2 C_{ph}$

where:

ρ = air density

V = wind speed (130 mph)

C_{ph} = 1.0 windward side (constant across surface)

= .40 leeward side (constant across surface)

These values of C_{ph} correspond to a drag coefficient of 1.4. In all the analyses, the pressures defined in this section were multiplied by a contingency factor of 1.15.

Teeter Brakes

Some form of teeter restraint is necessary to prevent impact into hard stops during abnormal operating conditions. Conditions are particularly severe during high wind shutdowns, with a yaw error. Comprehensive parametric studies led to the selection of a two-stage, friction brake system as protection for the rotor, because it introduced the minimum load into the system. The brake schedule is illustrated in Figure 29. During most of the operation, the teeter angle will be less than 2.5°, and the brakes will be totally disengaged. If for any reason the teeter angle exceeds ± 2.5° the first set of brakes will engage. This brake level can handle all but the most severe conditions. In the very few instances in which the teeter angle exceeds 5°, the full brake force will be applied and maintained and the system will be shut down. Transient dynamic analyses have shown that this brake system will keep operational teeter angles below 6°. When parked, the brakes are set at their highest level, to protect the system from dissymmetries in the oncoming wind. During startup, the high brake level is maintained until the rotor speed exceeds 6 rpm, then the schedule illustrated in Figure 29 is adopted for the remaining operation.

The supporting structure for the brake system is designed to 1.15 times the maximum brake level, or 2.76×10^6 ft.-lb.

Gearbox/Drivetrain

Special considerations were necessary in developing the fatigue spectrum for the gearbox design. Because the gear teeth are continually cycling between full load and no load, the absolute value of the torque governs the fatigue design. Therefore, a probability distribution of the sum of mean plus alternating rotor torques was developed. This distribution is referred to as the gearbox torque duty cycle.

The gearbox torque duty cycle is illustrated in Figure 30. Torque levels were normalized by the

rated value. The curves depict the load level probability of a sample taken at random during the 30 years of operation. Because certain of the fatigue loads, such as that caused by wind shear, reach a peak magnitude at a preferred rotor azimuth, the gears that are always in contact at a given rotor position (upper curve) must be distinguished from those that are not. In the first case the design is driven by the most highly loaded tooth, while in the second case the design takes advantage of the fact that load peaks are distributed among the many teeth.

The operation of the cycloconverter limits the maximum torque during normal operation to less than 1.3 times the rated value. Hence, the probability distributions may be truncated at this level for the purposes of gearbox fatigue design. The gearbox can withstand two times the rated torque as an extreme overload. This torque is much greater than the maximum anticipated torque for the system.

Other drive train components, such as shafting, used the interface torque loads which were presented in Figure 21 and Table 10.

STATISTICAL ANALYSIS OF MEASURED LOADS

In past NASA/DOE wind turbine programs, fatigue load test data has been reduced using a Type I statisitical analysis. Specifically, digitized waveforms are scanned and a maximum and minimum value are found during each rotor cycle. The maximum/minimum pairs are then used to compute mean and alternating loads for each rotor cycle. The alternating loads, in turn, are ordered from lowest to highest, and a probability distribution is thereby established. Since each rotor cycle is analyzed independently, the distributions found are consistent with the definition of Type I loads given earlier.

It is generally agreed that a Type I analysis alone is insufficient to predict fatigue damage for complex stress-strain time histories. Dowling (Reference 4) accesses various methods for counting fatigue cycles from irregular waveforms. He concluded that the "rainflow" or closely related "range-pair" method provides the best estimate of fatigue damage. In the rainflow technique, the maximum from one rotor cycle may combine with the minimum of another to yield a fatigue occurrence. The rainflow method, detailed in Reference 4, has been coded at General Electric for application to WTG data tapes.

Figure 31 compares MOD-2 blade flap bending data which has been processed by both the rainflow and standard Type I analysis techniques. Also shown are the shifts in mean loads assigned to Type II gust response. It is interesting to note that at the high probabilities, the rainflow loads are approximately equal to the Type I plus Type II amplitudes. In any event, it is clear that loads evaluation from Type I data alone can lead to unconservative conclusions. While existing wind statistics are insufficient to enable rainflow counting of theoretically predicted loads, the problem has been addressed at least in part on the MOD-5A by including Type II, Type IIA, and Type III cycles in the fatigue design load histograms. Reference to the combined Type I, II, and IIA distributions, in Figure 18, indicates a trend similar to the rainflow data.

CONCLUDING REMARKS

The following conclusions are drawn from this work:

1. Methods for the accurate prediction of transient limit loads are in place.
2. Test data supports the methods used for fatigue load prediction on the MOD-5A. It is important combine fatigue cycles due local turbulence with those due to global changes in mean wind speed. Statistical techniques to accomplish this have been presented and demonstrated in this paper. Additional research on local turbulence would be beneficial to increase confidence in and further quantify the model used. In particular, site-to-site differences, the spatial distribution of turbulence, and the phasing of turbulence harmonics could be profitably explored.
3. The rainflow method should be used to analyze wind turbine fatigue loads test data, in favor of current techniques.

REFERENCES

1. Pijawka, W.C., "Status of DOE/NASA MOD-5A Wind Turbine Project", to be published in the proceedings of the DOE/NASA Workshop on Horizontal Axis Wind Turbine Technology, held May 1984.

2. MOD-1 WIND TURBINE GENERATOR ANALYSIS AND DESIGN REPORT, Vol. 1, DOE/NASA/0058-79/2, NASA CR-159495, May 1979.

3. Kubar, E.J., "Selected System Modes Using the Dynamic Transformation with Modal Synthesis", Shock and Vibration Bulletin, August 1974, pp. 91-102.

4. Dowling, N.E., "Fatigue Failure Predictions for Complicated Stress-Strain Time Histories", Journal of Materials, JMLSA, Vol. 7, No. 1, March 1972, pp. 71-87.

ACKNOWLEDGEMENTS

This work was performed under contract DEN 3-153 with NASA-Lewis Research Center. The authors would like to express their particular thanks to David A. Spera and Timothy L. Sullivan of the NASA Wind Energy Project Office for their support throughout the program.

Table 1 Classification of Wind Models

I WIND MODELS FOR LIMIT LOADS
1. Hurricane - per MOD-5A SOW
2. Large Rotor Enveloping Gusts (99.99%'ile)
3. Yaw Misalignments
4. Wind Shear - per MOD-5A SOW

II WIND MODELS FOR FATIGUE LOADS
1. Yearly Mean Wind Distribution - Weibull per MOD-5A SOW
2. Mean Wind Variations
3. Large Rotor Enveloping Gusts (Up to 99.9%'ile)
   Note: Same as Model I.2.
4. Local Turbulence - per NASA Interim Turbulence Model
5. Tower Shadow - per Potential Flow Theory for Upwind Rotor
6. Wind Shear - per MOD-5A SOW

Table 2 Formulas for the Wind Turbulence Model

$$V_{TURB}(X, \psi, P) = X \sum_{i=1}^{6} V_{RMS_i} \cos i(\psi + \phi i) \sqrt{-2 \ln (1-P)}$$

where

V_{TURB} = Wind speed variation due to turbulence
X = Non-dimensional blade spanwise station
P = Probability that turbulence input is less than or equal to V_{TURB}
V_{RMSi} = RMS of turbulence velocity at the i^{th} rotor harmonic per NASA Interim Turbulence Model
i = Rotor harmonic
ψ = Rotor blade angular position
ϕi = Phase of i^{th} harmonic (set = constant for MOD-5A analysis - theoretically random)

$$V_{RMS_i} = \frac{\Delta V_S}{2\sqrt{2}} \frac{1}{i + .75}$$

ΔV_S = Difference in wind speed between the highest and lowest points in the rotor disc as predicted by the wind shear model in the MOD-5A SOW.

Table 3 MOD-5A System Natural Frequencies

		VERTICAL		HORIZONTAL		HARMONICS
		Hz	P	Hz	P	TO AVOID
1)	DRIVE TRAIN	0.		0.		E
2)	TEETER	.28 (.23)	1. (1.)	.28 (.23)	1. (1.)	-
3)	TOWER Z	.340	1.21 (1.48)	.340	1.21 (1.48)	E
4)	TOWER Y	.341	1.22 (1.48)	.344	1.23 (1.50)	E
5)	FLAP COLLECTIVE	1.17	4.18 (5.00)	1.17	4.18 (5.00)	E
6)	DRIVE TRAIN	1.33	4.75 (5.78)	1.33	4.75 (5.78)	E
7)	CHORD CYCLIC	1.60	5.71 (6.96)	1.84	6.57 (8.00)	O
8)	FLAP CYCLIC	2.37	8.46 (10.3)	2.3	8.25 (9.96)	O
9)	TOWER C-L TORSION	2.24	8.00 (9.74)	1.80	6.43 (7.83)	E
10)	TOWER Z (2nd)	3.03	10.8 (13.2)	3.23	11.7 (14.0)	E
11)	FLAP COLLECTIVE (2nd)	3.14	11.2 (13.6)	3.11	11.1 (13.4)	E
12)	CHORD COLLECTIVE	4.08	14.6 (17.7)	4.08	14.6 (17.7)	E
13)	TOWER Y (2nd)	4.18	14.9 (18.2)	4.18	14.9 (18.2)	E
14)	FLAP CYCLIC (2nd)	4.56	16.3 (19.7)	4.56	16.3 (19.7)	O

* Per rev nos. in parenthesis are for 13.8 rpm

E = even
O = odd

Table 4 MOD-5A Wind Bin and Fatigue Cycle Summary

BIN	MID-POINT (MPH @ HUB)	RANGE (MPH)	NOMINAL RPM	NO. OF FATIGUE CYCLES PER 30 YEARS TYPE I	TYPE II	TYPE IIA	TYPE III
1	16.5	14 - 19	13.8	92.7E6	4.05E6	.365E6	---
2	21.5	19 - 24	13.8	93.5E6	4.08E6	.368E6	---
3	26.0	24 - 28	16.8	71.3E6	2.55E6	.230E6	---
4	31.5	28 - 35	16.8	66.5E6	2.37E6	.214E6	---
5	40.0	35 - 45	16.8	19.2E6	.68E6	.062E6	---
6	52.5	45 - 60	16.8	.86E6	.03E6	2800.	---
TOTAL				344.E6	13.8E6	1.24E6	35000.

NOTES: FATIGUE CYCLES BASED ON .96 AVAILABILITY
TYPE 1 CYCLES BASED ON 2P OCCURRENCE RATE

Table 5a Amplitude of Large Rotor Enveloping Gusts Used for Type II and Limit Loads

BIN	V_{MEAN} (MPH)	ΔV = TOTAL GUST MAGNITUDE (MPH) FOR %'ILE 40%	86%	99%	99.9%	99.99%
1	16.5	1.83	3.60	5.51	6.75	7.79
2	21.5	2.39	4.69	7.18	7.79	10.2
3	26.0	2.89	5.67	8.68	10.6	12.3
4	31.5	3.50	6.87	10.5	12.9	14.9
5	40.0	4.45	8.73	13.4	16.4	18.9
6	52.5	5.84	11.45	17.5	21.5	24.8

$\Delta V = .11\ V_{MEAN} \sqrt{-2 \ln (1-P)}$, $P = \%/100$

V RANGE = V_{MEAN} TO $(V_{MEAN} + \Delta V)$ FOR UPGUSTS
V RANGE = $(V_{MEAN} - \Delta V)$ TO V_{MEAN} FOR DOWNGUSTS

Table 5b Amplitudes of Mean Wind Shifts Used for Type IIA Loads

BIN	V_{MEAN} (MPH)	ΔV = ± SHIFT MAGNITUDE (MPH) FOR %'ILE 40%	86%	99%	99.9%
1	16.5	1.33	2.62	4.01	4.91
2	21.5	1.74	3.41	5.22	6.39
3	26.0	2.10	4.12	6.31	7.73
4	31.5	2.55	5.00	7.65	9.37
5	40.0	3.23	6.35	9.71	11.9
6	52.5	4.25	8.33	12.8	15.6

$\Delta V = .08\ V_{MEAN} \sqrt{-2 \ln (1-P)}$

V RANGE = $(V_{MEAN} - \Delta V)$ TO $(V_{MEAN} + \Delta V)$ FOR ALL SHIFTS

Table 6 Critical Limit Load Conditions

CONDITION	COMMENTS
1. HURRICANE (130 MPH @ HUB)	TOWER BENDING AND FOUNDATION CRITICAL
2. CONTROL HARDWARE FAILURE (60 MPH, 0° AILERON ANGLE)	INBOARD BLADE/ROTOR CRITICAL
3. 99.99%'ILE GUST AT RATED WIND SPEED, 25% OVERSPEED, DESYNCRONIZATION AND SHUTDOWN	OUTBOARD BLADE CRITICAL
4. SHUTDOWN @ CUT-OUT WIND SPEED WITH YAW ERROR	SETS DESIGN REQUIREMENTS FOR TEETER BRAKES
5. 50% OVERSPEED, HIGH WIND ADVERSE AILERON SETTING	SURVIVAL CONDITION, SYSTEM DESIGNED TO PREVENT CATASTROPHIC FAILURE

Table 7 ADDITIONAL TRANSIENT EVENTS ANALYZED

CONDITION	COMMENTS
1. GUSTS/SHUTDOWNS @ WIND SPEEDS OTHER THAN RATED	GUST @ RATED WIND SPEED PRODUCED LARGEST LOADS
2. ONE SET OF AILERONS STUCK (i.e MISMATCH BETWEEN THE 2 BLADES)	o LOADS NOT CRITICAL DUE TO TEETERING RELIEF o SUFFICIENT ROTOR/TOWER CLEARANCES o SUFFICIENT BRAKING TORQUE ON ONE BLADE FOR SHUTDOWN
3. 180° SHIFT IN WIND DIRECTION WITHIN 10 SECONDS	LOADS/MOTIONS NOT CRITICAL
4. START UP/SHUTDOWN THROUGH TOWER RESONANCE	MOD-5A CONTROL SYSTEM AVOIDS DWELL AT RESONANCE. LOADS NOT CRITICAL

TABLE 8 SYSTEM INTERFACES

Reference	Location	Comment
1	.90R	
2	.80R	
3	.70R	
4	.60R	Main Blade Station
5	.50R	
6	.40R	
7	.30R	
8	.25R	
9	.20R	
10	.10R	
11	.0R	
12	Teeter Bearing	Rotating System
13	Rotor - CL	Center of Teeter Bearing Non-rotating
14	Rotor/Nacelle	
15	Yaw Bearing	
16	Tower 185	(Feet Above ground)
17	Tower 117	
18	Tower 51	(Tower knuckle)
19	Tower base	
20	Ailerons	Load/span from .60R to .99R

Table 9 Typical Load Histogram Presentation

CUMULATIVE FATIGUE HISTOGRAM OUTPUT

TOWER BASE MZ

		HALF-RANGE FATIGUE LOADS			CORRESPONDING MID-RANGE LOAD DISTRIBUTION			
NO. CYCLES IN 30 YEARS (TYPES 1+2)	CUM PROB	LOAD LEVELS	NORMALIZED LOAD LEVELS	LOAD/50% AT RATED	MEAN	STANDARD DEVIATION	MAXIMUM	MINIMUM
0.	0.	0. - 0.178E 06	0. - 0.03	0. - 0.08	0.	0.	0.	0.
0.	0.	0.178E 06 - 0.357E 06	0.03 - 0.07	0.08 - 0.15	0.	0.	0.	0.
0.	0.	0.357E 06 - 0.535E 06	0.07 - 0.10	0.15 - 0.23	0.	0.	0.	0.
0.	0.	0.535E 06 - 0.713E 06	0.10 - 0.14	0.23 - 0.31	0.	0.	0.	0.
0.	0.	0.713E 06 - 0.891E 06	0.14 - 0.17	0.31 - 0.38	0.	0.	0.	0.
0.	0.	0.891E 06 - 0.107E 07	0.17 - 0.20	0.38 - 0.46	0.	0.	0.	0.
0.	0.	0.107E 07 - 0.125E 07	0.20 - 0.24	0.46 - 0.54	0.	0.	0.	0.
0.	0.	0.125E 07 - 0.143E 07	0.24 - 0.27	0.54 - 0.62	0.	0.	0.	0.
0.	0.	0.143E 07 - 0.160E 07	0.27 - 0.30	0.62 - 0.69	0.	0.	0.	0.
0.764E 06	0.00213	0.160E 07 - 0.178E 07	0.30 - 0.34	0.69 - 0.77	-0.317E 07	0.480E 06	-0.192E 07	-0.335E 07
0.516E 07	0.01650	0.178E 07 - 0.196E 07	0.34 - 0.37	0.77 - 0.85	-0.307E 07	0.574E 06	-0.192E 07	-0.347E 07
0.171E 08	0.06416	0.196E 07 - 0.214E 07	0.37 - 0.41	0.85 - 0.92	-0.295E 07	0.649E 06	-0.192E 07	-0.347E 07
0.320E 08	0.15338	0.214E 07 - 0.232E 07	0.41 - 0.44	0.92 - 1.00	-0.282E 07	0.698E 06	-0.192E 07	-0.347E 07
0.482E 08	0.28771	0.232E 07 - 0.254E 07	0.44 - 0.48	1.00 - 1.10	-0.269E 07	0.733E 06	-0.131E 07	-0.347E 07
0.390E 08	0.39639	0.254E 07 - 0.277E 07	0.48 - 0.53	1.10 - 1.20	-0.248E 07	0.798E 06	-0.457E 06	-0.347E 07
0.278E 08	0.47380	0.277E 07 - 0.300E 07	0.53 - 0.57	1.20 - 1.29	-0.196E 07	0.905E 06	-0.457E 06	-0.347E 07
0.302E 08	0.55802	0.300E 07 - 0.322E 07	0.57 - 0.61	1.29 - 1.39	-0.134E 07	0.743E 06	-0.457E 06	-0.347E 07
0.377E 08	0.66305	0.322E 07 - 0.345E 07	0.61 - 0.66	1.39 - 1.49	-0.105E 07	0.560E 06	-0.457E 06	-0.347E 07
0.414E 08	0.77822	0.345E 07 - 0.368E 07	0.66 - 0.70	1.49 - 1.59	-0.937E 06	0.486E 06	-0.337E 06	-0.347E 07
0.364E 08	0.87972	0.368E 07 - 0.391E 07	0.70 - 0.74	1.59 - 1.69	-0.793E 06	0.441E 06	-0.135E 06	-0.347E 07
0.228E 08	0.94334	0.391E 07 - 0.413E 07	0.74 - 0.78	1.69 - 1.78	-0.703E 06	0.419E 06	-0.155E 06	-0.347E 07
0.117E 08	0.97582	0.413E 07 - 0.436E 07	0.78 - 0.83	1.78 - 1.88	-0.659E 06	0.384E 06	0.394E 05	-0.347E 07
0.537E 07	0.99076	0.436E 07 - 0.459E 07	0.83 - 0.87	1.88 - 1.98	-0.613E 06	0.347E 06	-0.284E 06	-0.347E 07
0.217E 07	0.99679	0.459E 07 - 0.481E 07	0.87 - 0.91	1.98 - 2.08	-0.575E 06	0.309E 06	-0.457E 06	-0.347E 07
0.797E 06	0.99901	0.481E 07 - 0.504E 07	0.91 - 0.96	2.08 - 2.17	-0.569E 06	0.303E 06	-0.457E 06	-0.347E 07
0.322E 06	0.99990	0.504E 07 - 0.527E 07	0.96 - 1.00	2.17 - 2.27	-0.457E 06	0.453E 02	-0.457E 06	-0.457E 06

TOTAL CYCLES = 0.359E 09

ROOT MEAN CUBED IS 0.322E 07 AVERAGE MEAN IS -0.172E 07

Table 10 Normalized Fixed System Limit Load Summary

CONDITION	ROTOR TORQUE / RATED TORQUE	RESULTANT BENDING/1G ROTOR/NACELLE	RESULTANT BENDING/1G YAW BEARING	RESULTANT BENDING @ TOWER BASE*
HURRICANE	---	1.0	1.80	2.35
CONTROLS FAILURE @ 60 MPH	1.39	1.57	.60	1.91
99.99% GUST @ RATED	1.26	1.44	.60	1.93
SHUTDOWN @ CUT-OUT WITH YAW ERROR	NOT CRITICAL	1.85	1.22	NOT CRITICAL
CYCLOCONVERTER MISHAP	1.73	---	---	---

* Normalized by bending moment due to rotor aerodynamic thrust at rated wind speed.

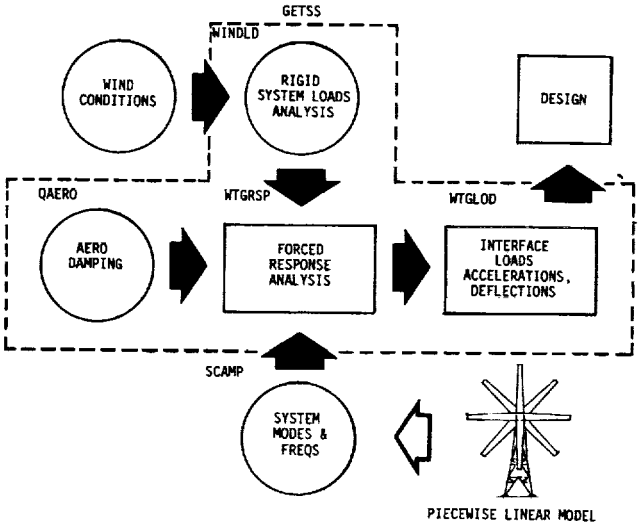

Figure 1. GETSS Analysis Flow

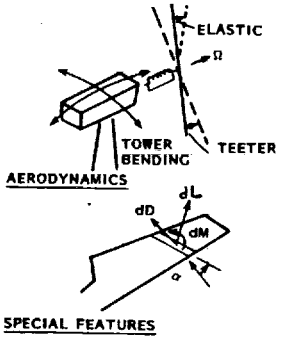

° FREEDOM
- TEETER
- ROTOR SPEED
- 3 ELASTIC FLAP MODES/BLADE
- TOWER BENDING 2-DIRECTION
- CONTROL SYSTEM

- TABLE LOOKUP, C_L, C_D, C_M, vs α
- QUASI-STEADY AERODYNAMICS
- STALL DELAY AS F'N OF °
- MOMENTUM THEORY DOWNWASH

SPECIAL FEATURES
- V, YAW ↓, CONTROL ↓ vs TIME INPUTS
- DESYNCH @ PRESCRIBED TIME OR POWER LEVEL
- TEETER BRAKE/STOPS DYNAMICS

OUTPUT
TIME HISTORIES OF LOADS AND MOTIONS

Figure 2. Features of the TRAC Code

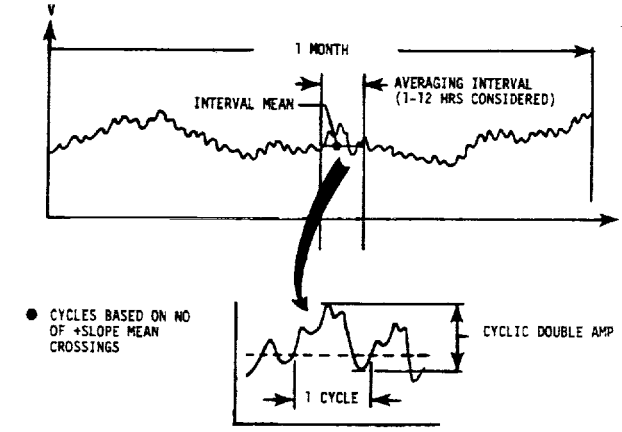

Figure 3. Development of Mean Wind Variation Model

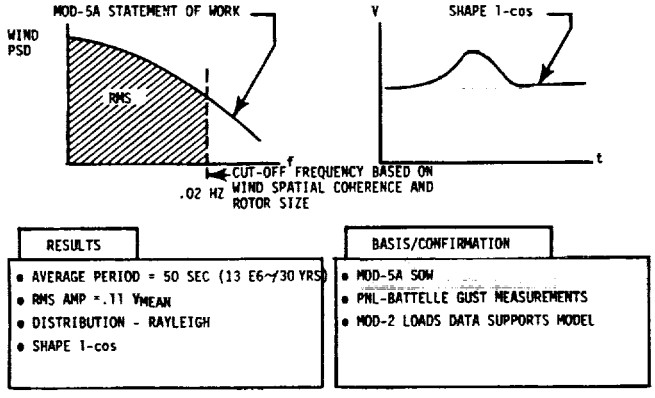

Figure 4. Development of Large Rotor-Enveloping Gust Model

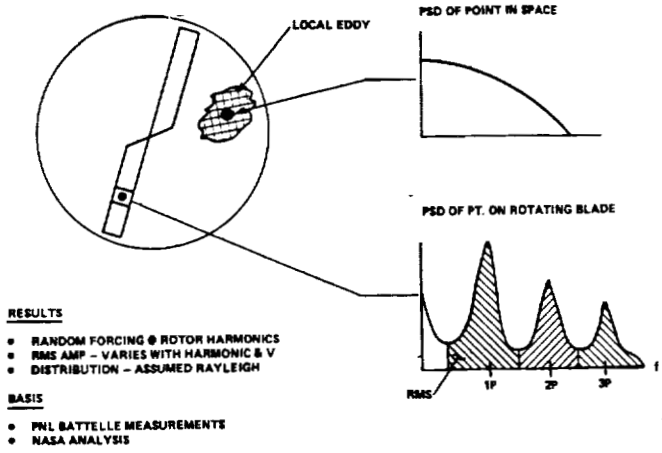

Figure 5. Development of Local Turbulence Wind Model

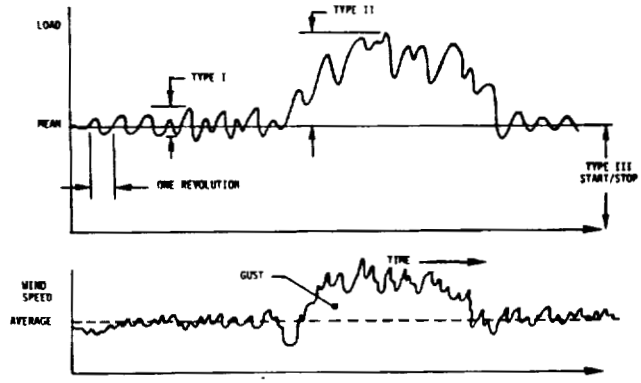

Figure 6. Fatigue Load Types

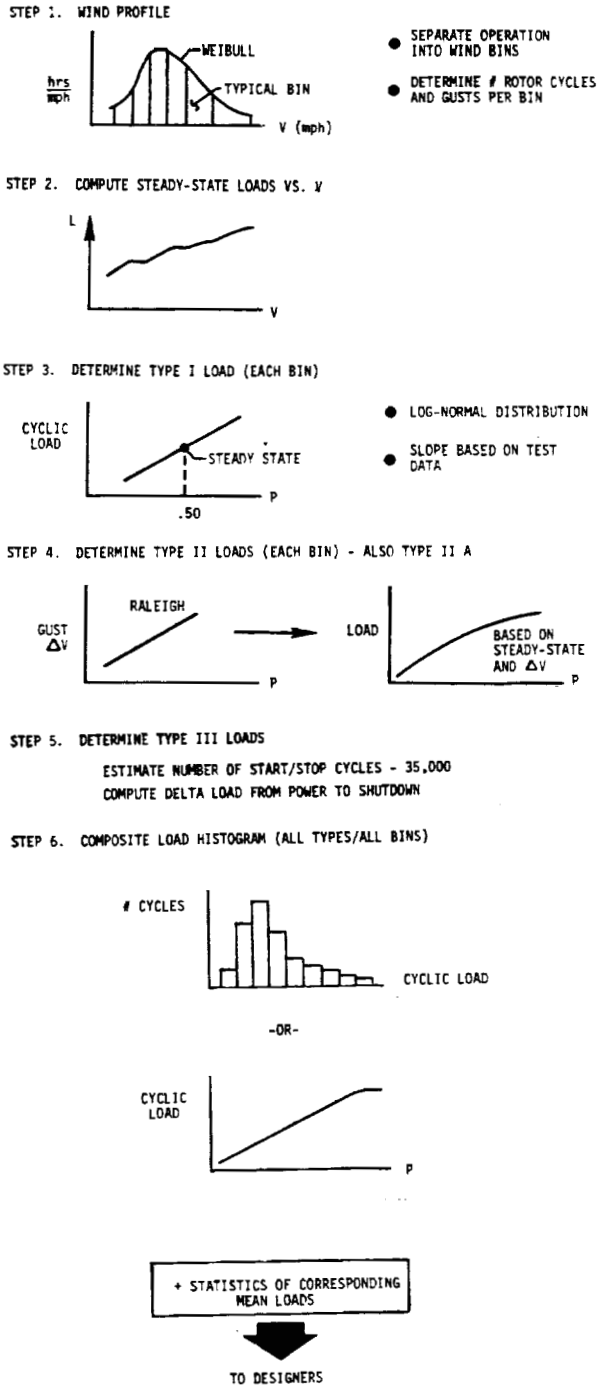

Figure 7. Procedure for Determining Life Cycle Fatigue Loads

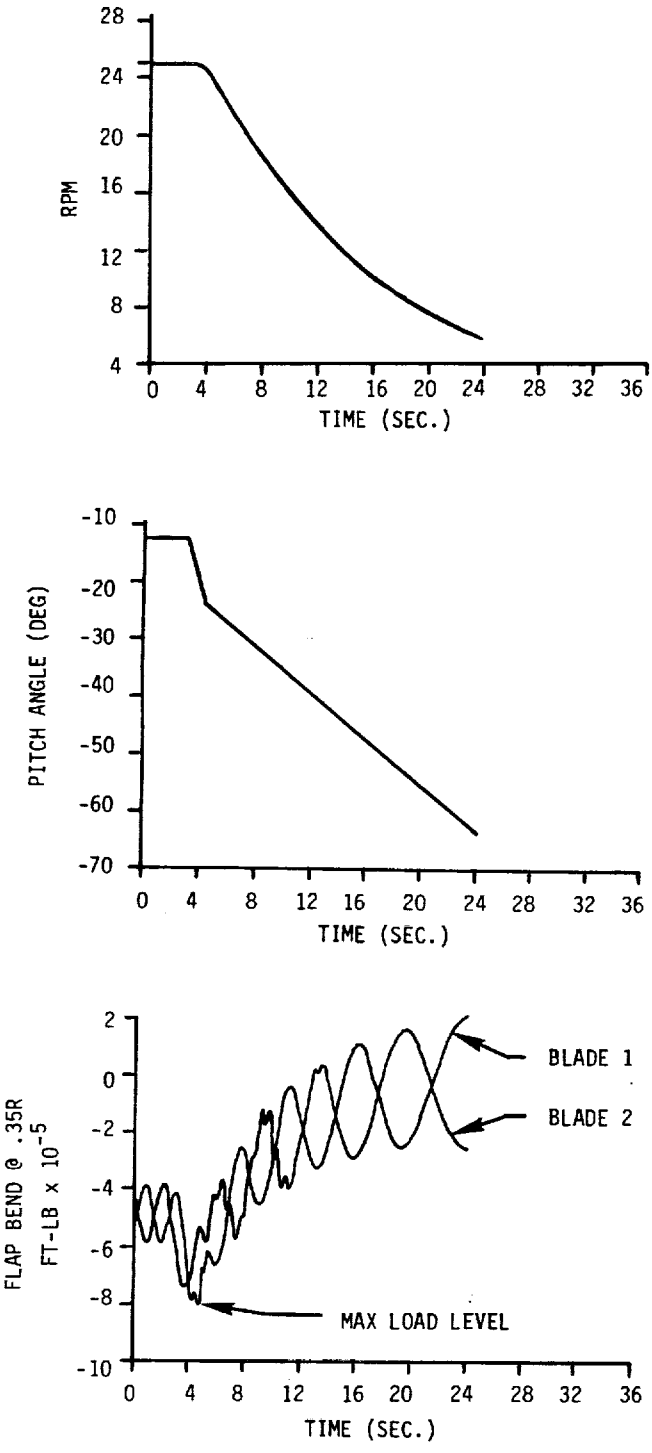

Figure 8. Simulation of MOD-1 Shutdown Using the TRAC Code

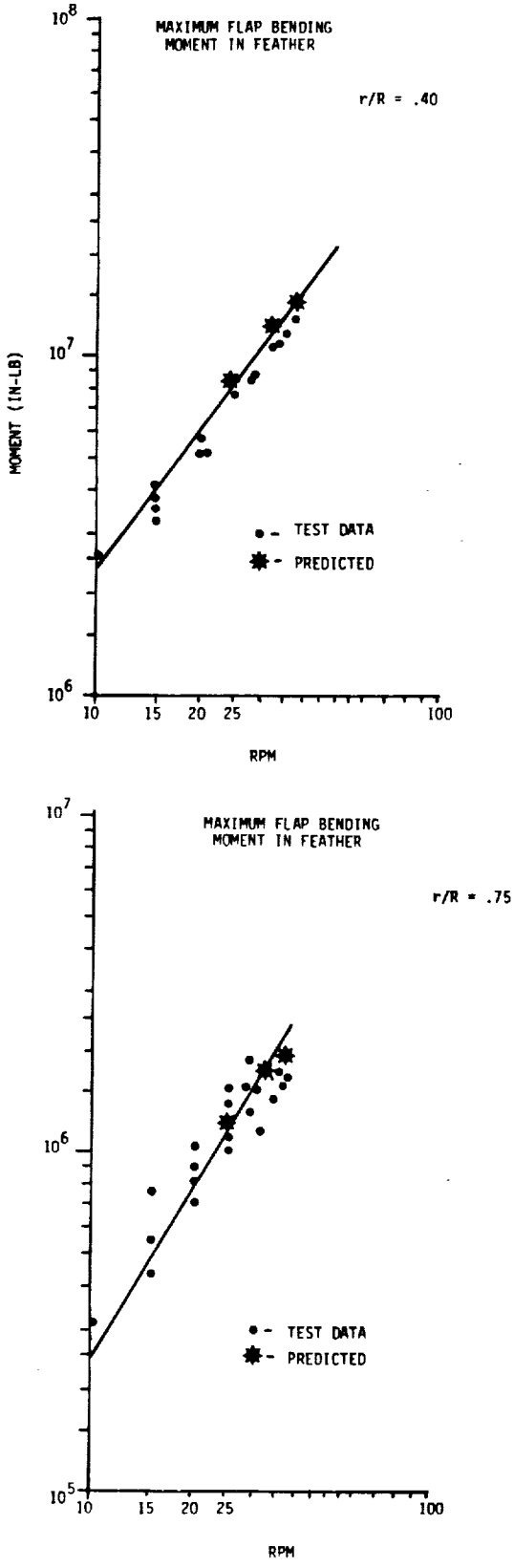

Figure 9. Comparison of MOD-1 Shutdown Test Blade Loads with Theoretical Predictions

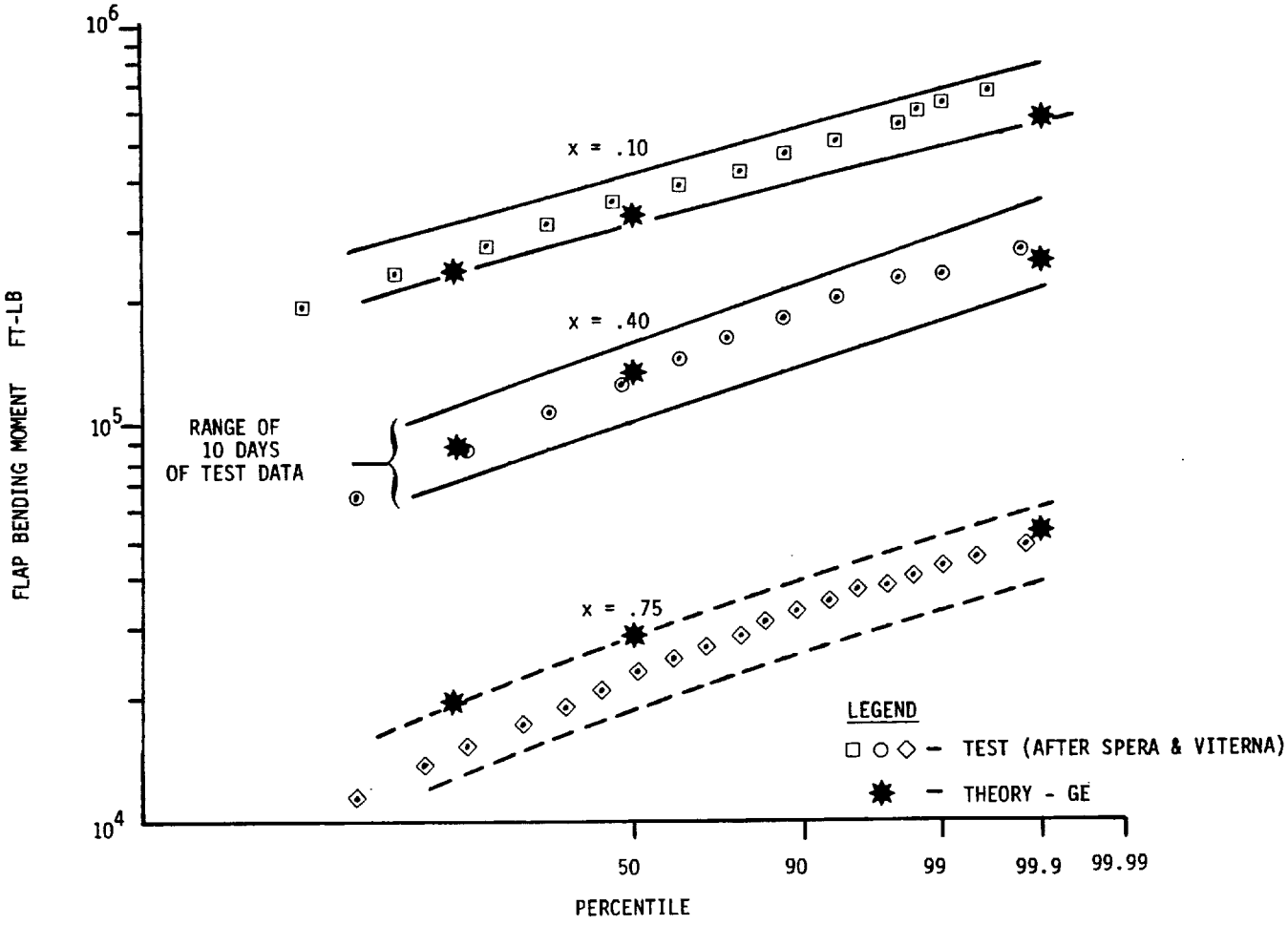

Figure 10. Test/Theory Correlation of MOD-1 Type I Fatique Loads

# CYCLES/HOUR			
HOUR	V @ 195	FLAP BENDING .20R	FLAP BENDING .65R
1	76	40	63.8
2	81.5	86.5	64.5
3	78.1	46.5	53.1
4	78.1	59.4	87.7
5	95.6	42.1	36.6
AVG	81.9	54.9	61.1

MOD-5A Prediction 65 Cycles/Hr

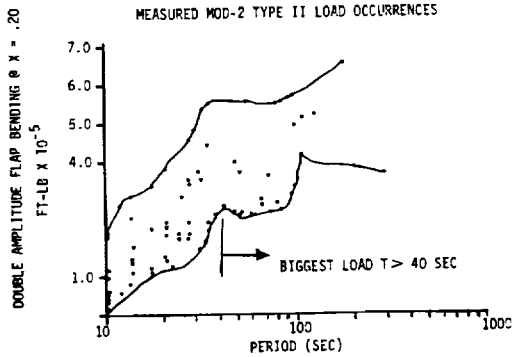

Figure 11. Frequency of Occurance of MOD-2
Type II Load Measurements

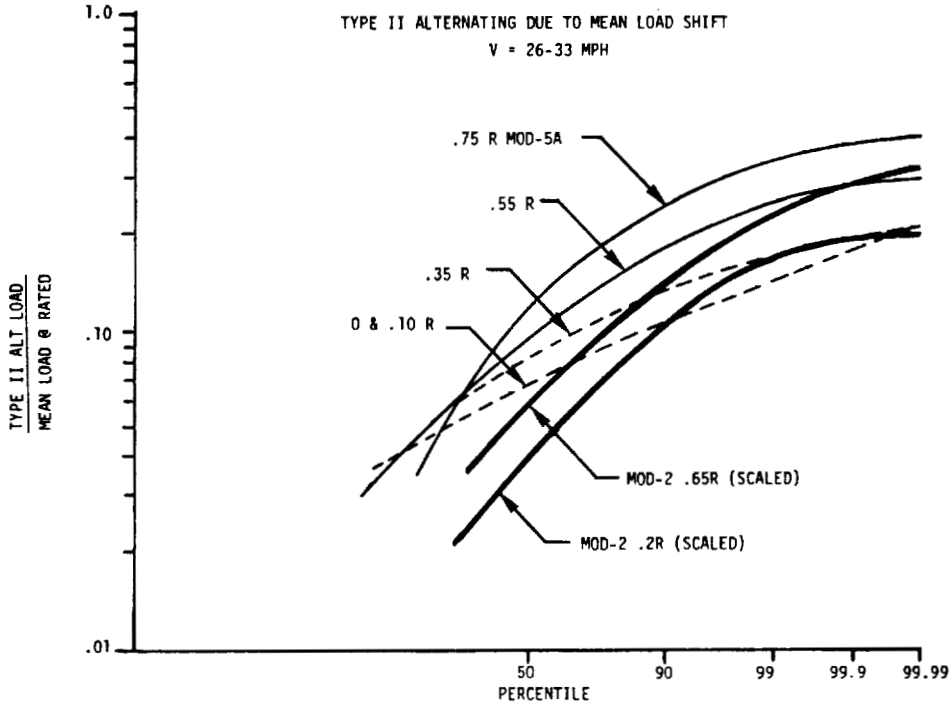

Figure 12. Comparison of MOD-5A Type II Load Predictions with Scaled MOD-2 Measurements

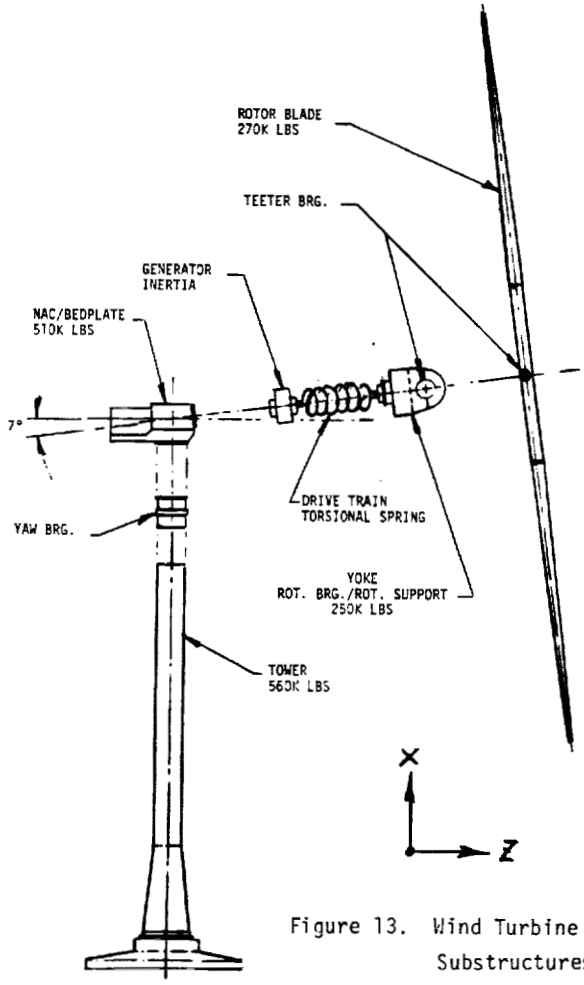

Figure 13. Wind Turbine Model Substructures

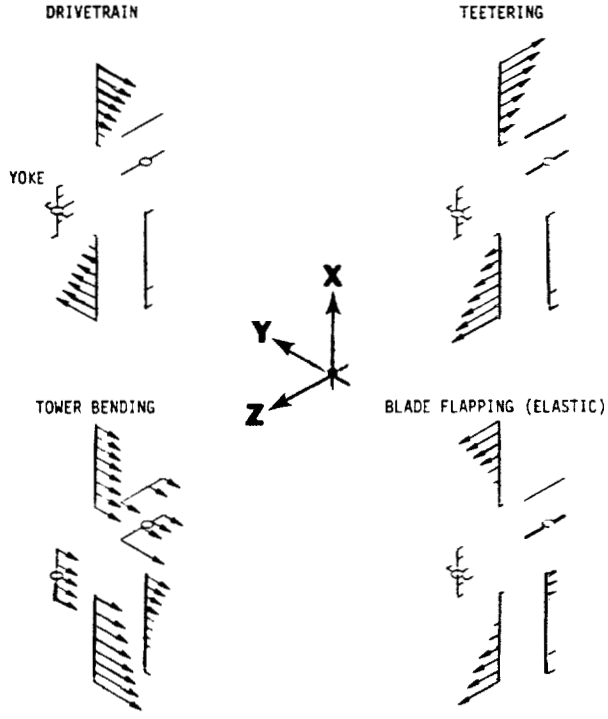

Figure 14. Coupled Mode Shapes

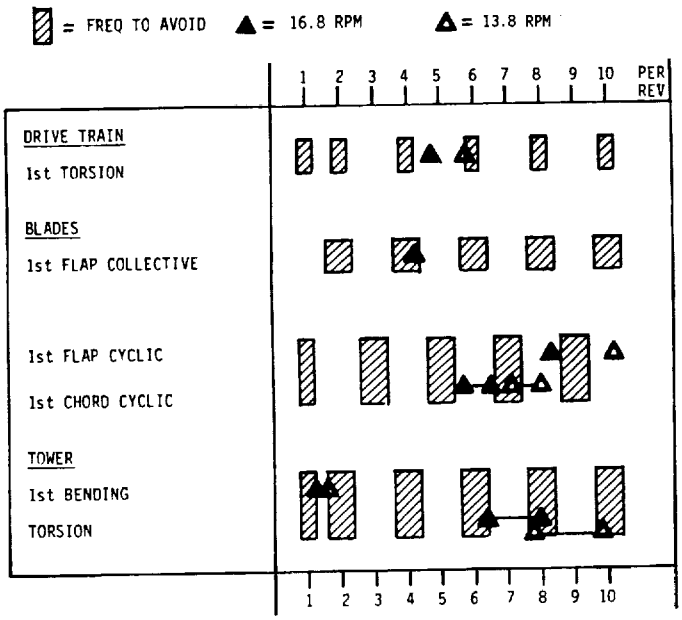

Figure 15. MOD-5A Natural Frequency Placement

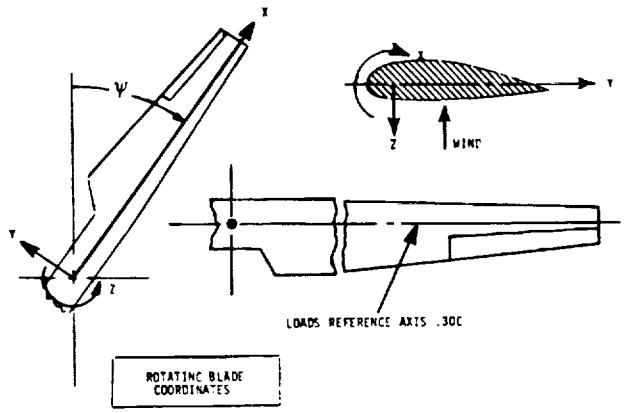

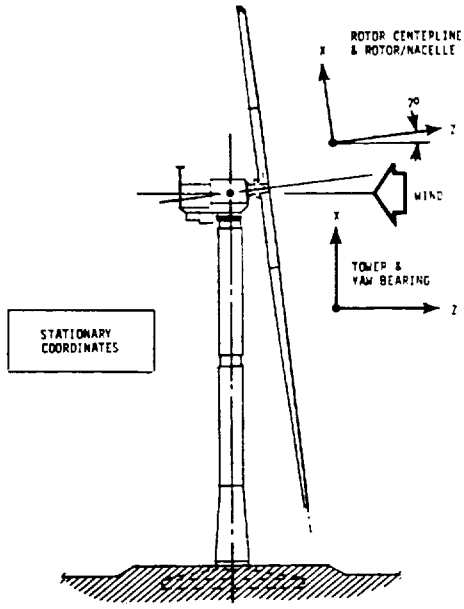

Figure 16. Sign Conventions

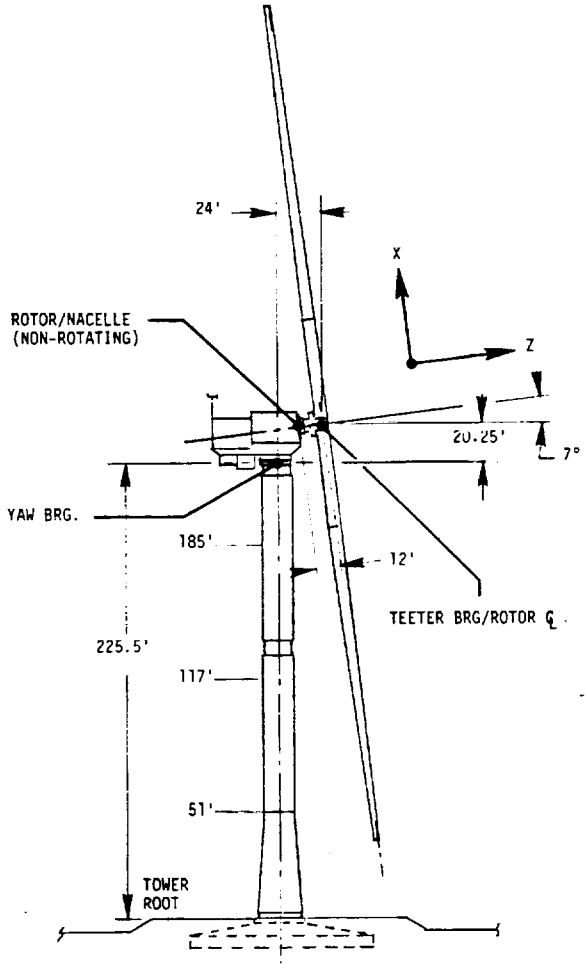

Figure 17. System Dimensions and Interfaces

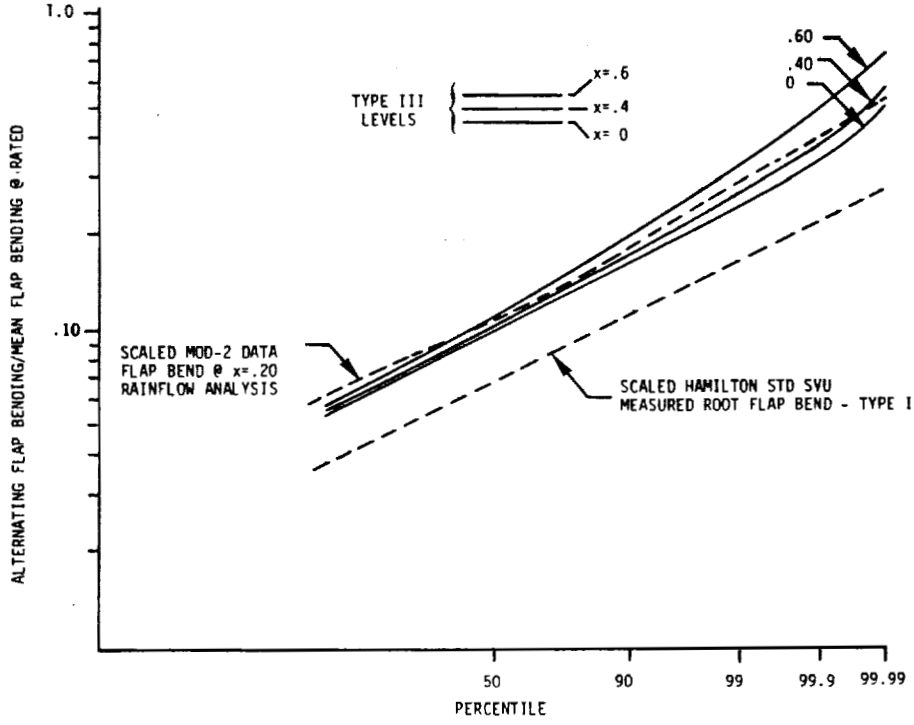

Figure 18. Blade Flapwise Bending Moment Probability Distributions

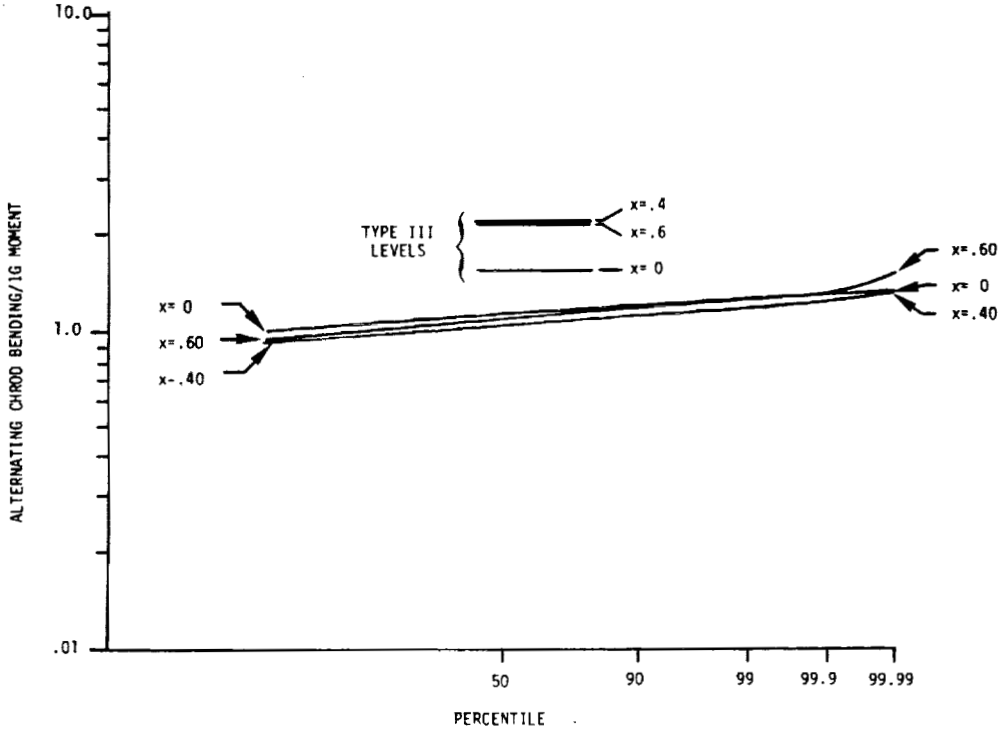

Figure 19. Blade Chordwise Bending Moment Probability Distributions

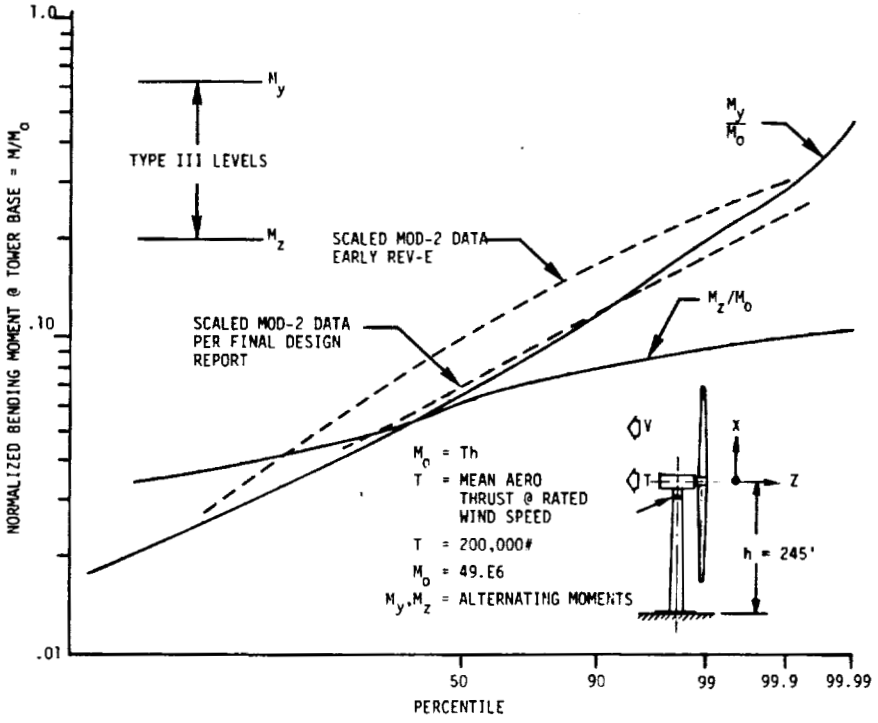

Figure 20. Tower Root Bending Moment Probability Distributions

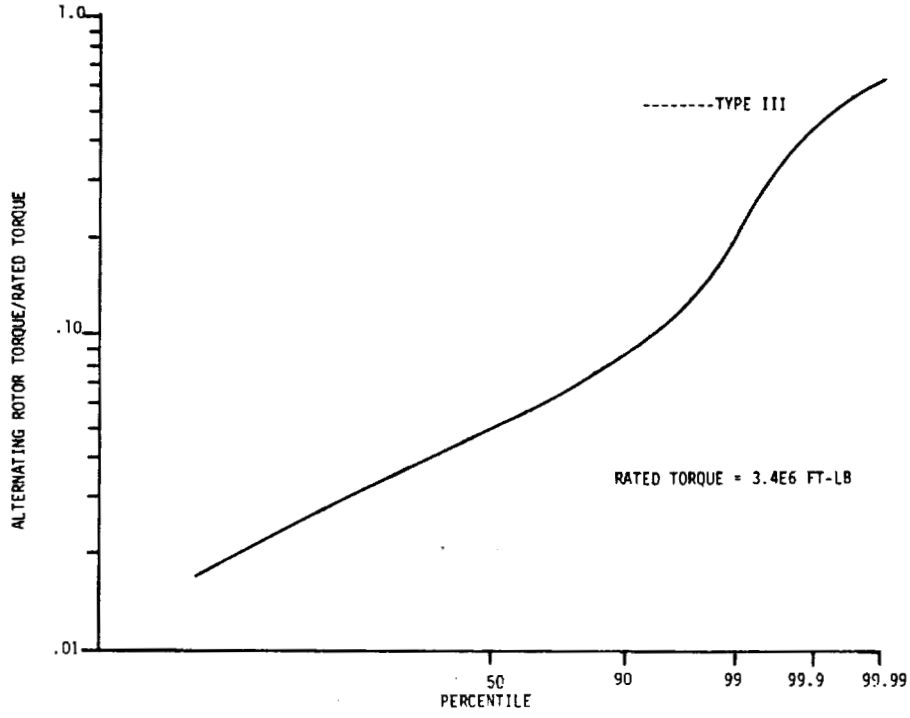

Figure 21. Rotor Torque Probability Distribution

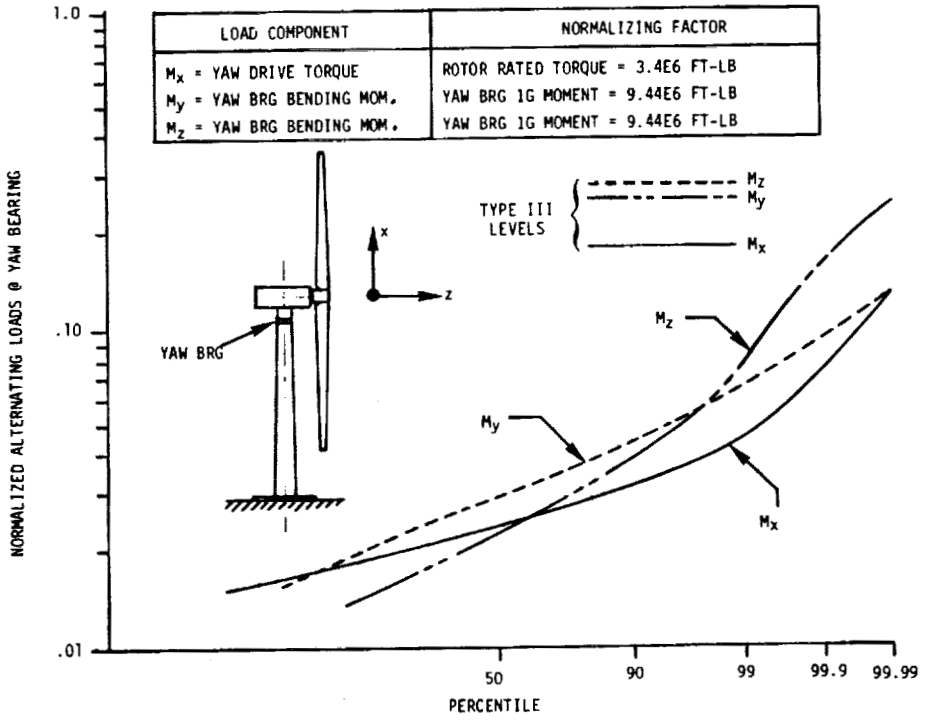

Figure 22. Yaw Bearing Bending Moment and Drive Torque Probability Distributions

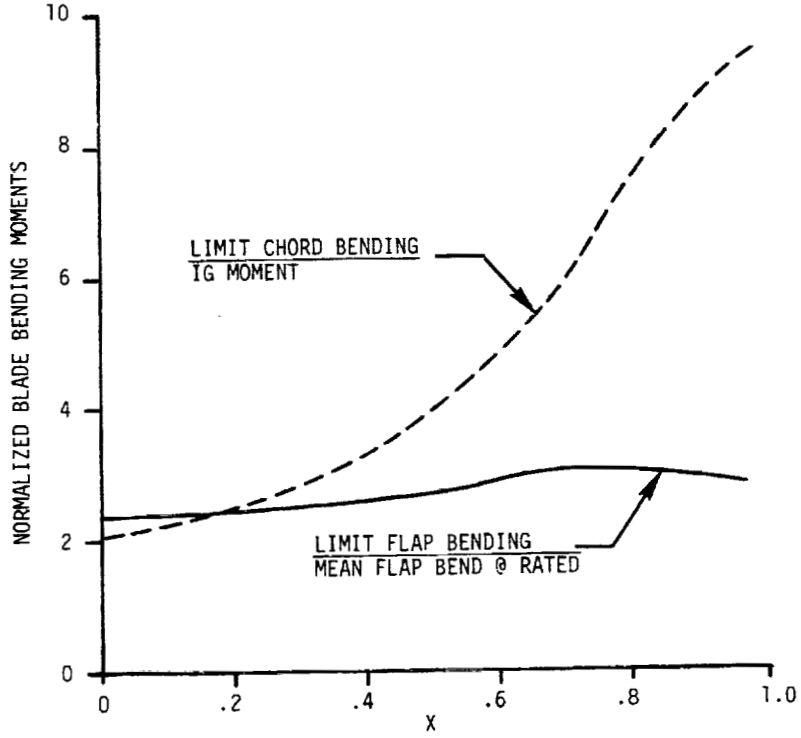

Figure 23. Blade Limit Loads

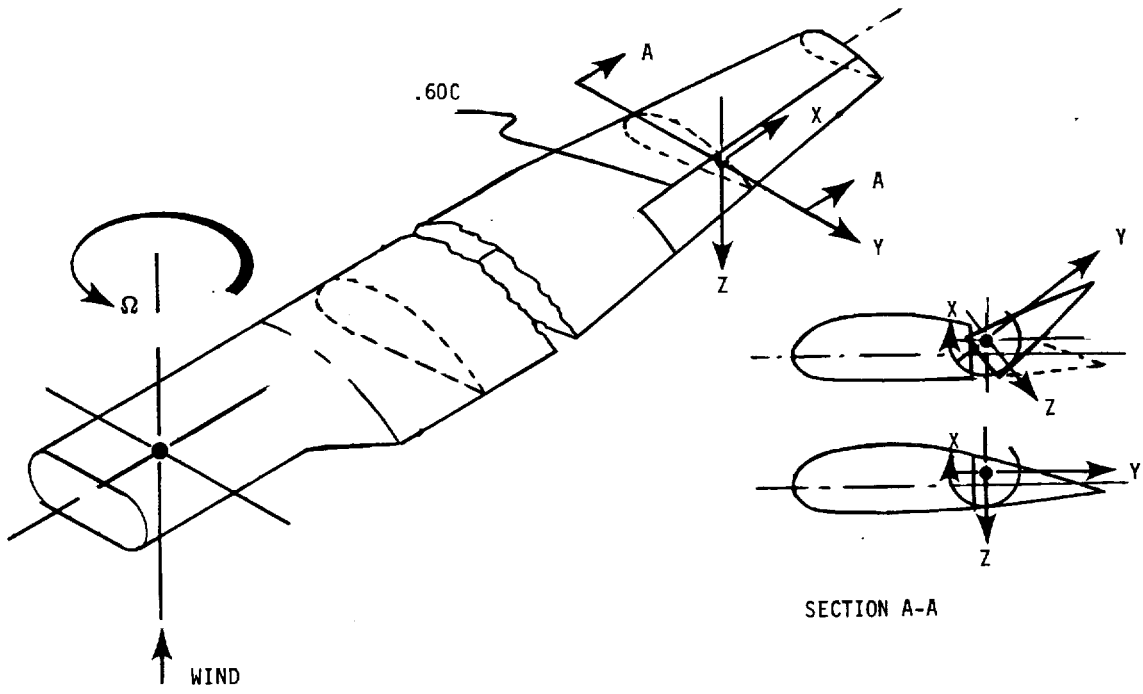

Figure 24. Aileron Coordinate System

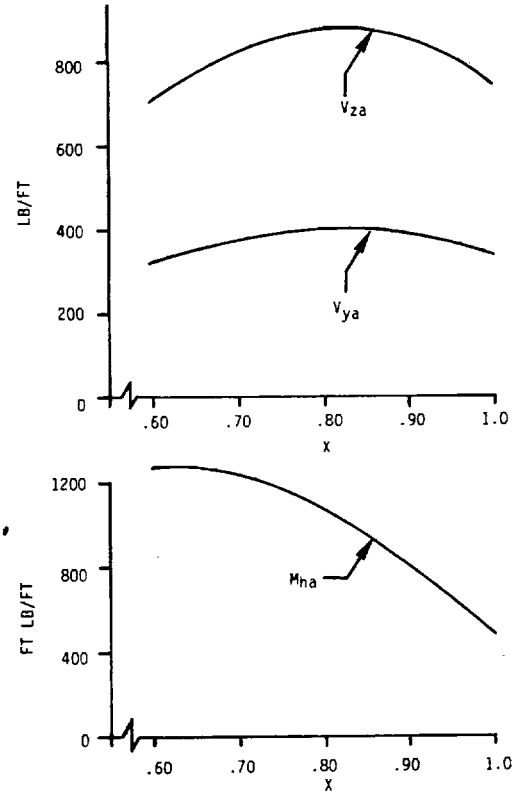

Figure 25. Aileron Aerodynamic Limit Loads for a 25% Overspeed Condition. Ailerons Deflected 45°.

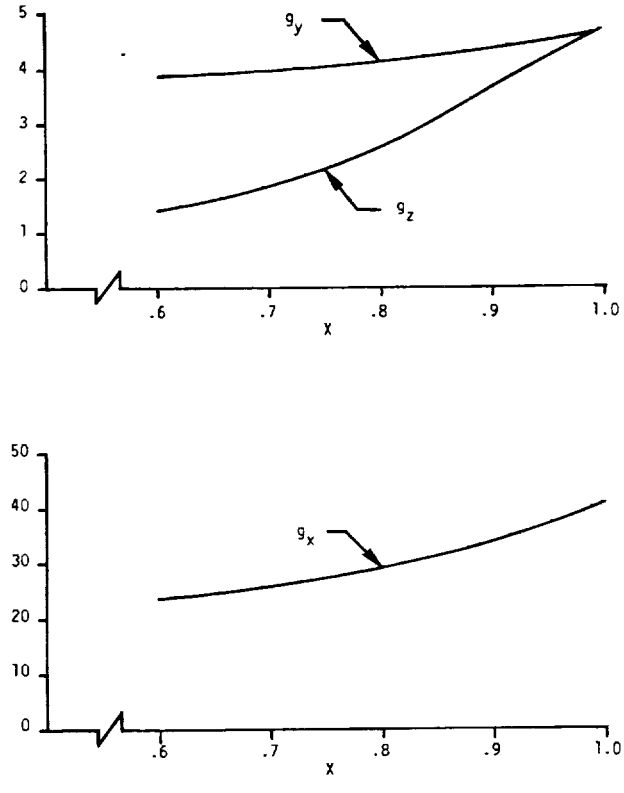

Figure 26. Aileron Inertial Limit Loads for a 25% Overspeed Condition. Ailerons Deflected 45°.

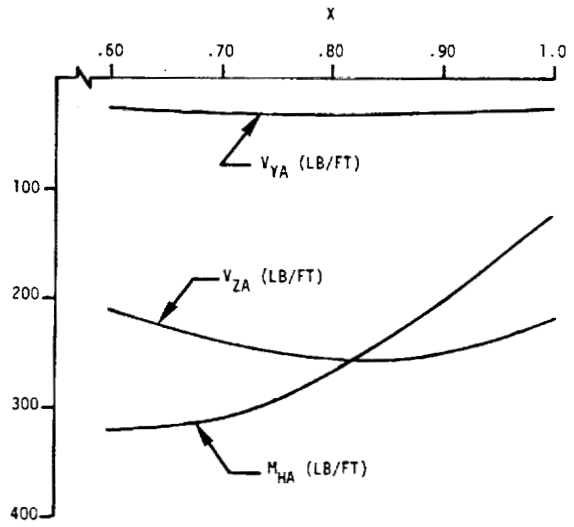

Figure 27. Mean Aerodynamic Aileron Loads at Rated Wind Speed. Fiftieth (50th) Percentile Cyclic Loads are 15% of Shown Mean Loads

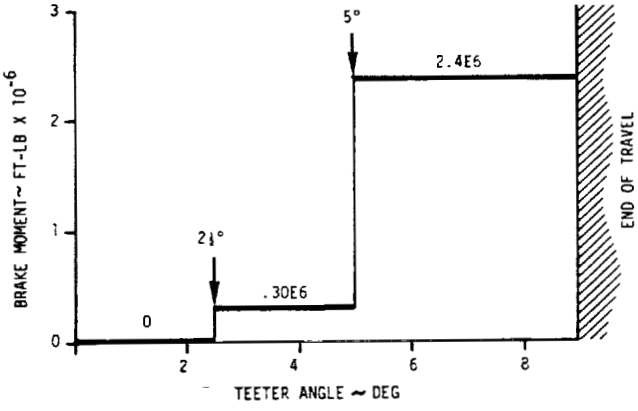

Figure 29. MOD-5A Teeter Brake Schedule

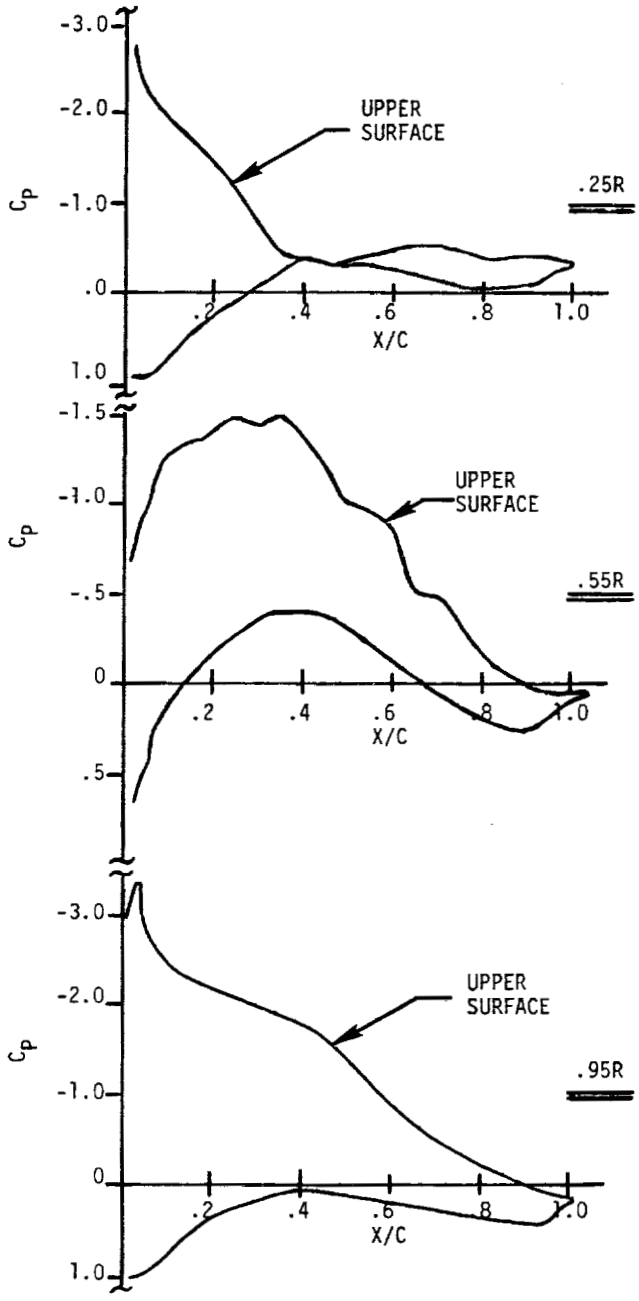

Figure 28. Airfoil Pressure Coefficients. Shown for Sections at x=.25, .55, and .95

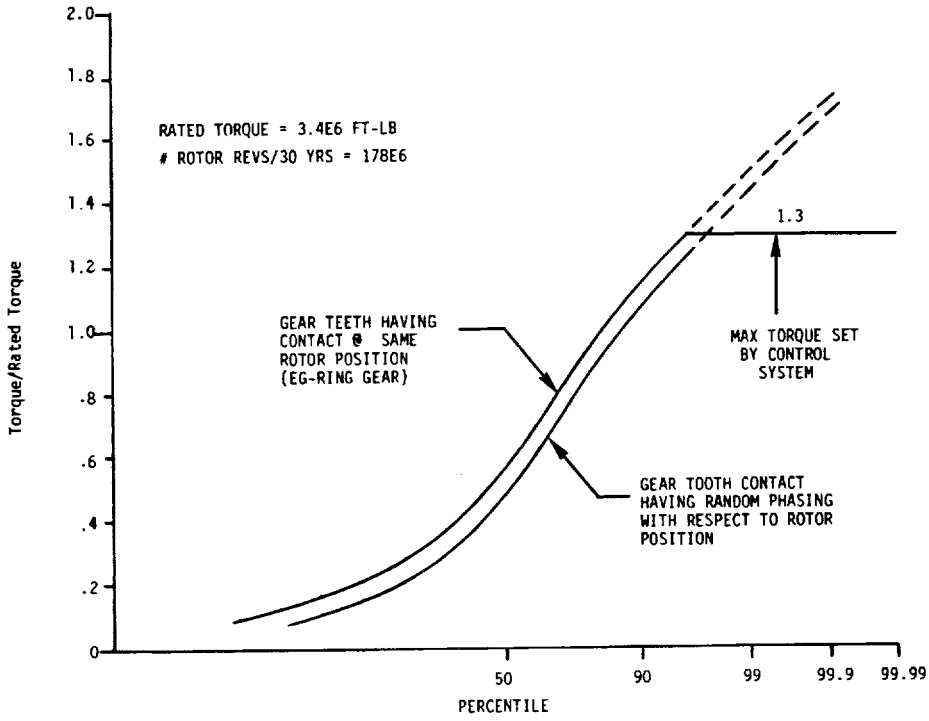

Figure 30. MOD-5A Gearbox Torque Duty Cycle

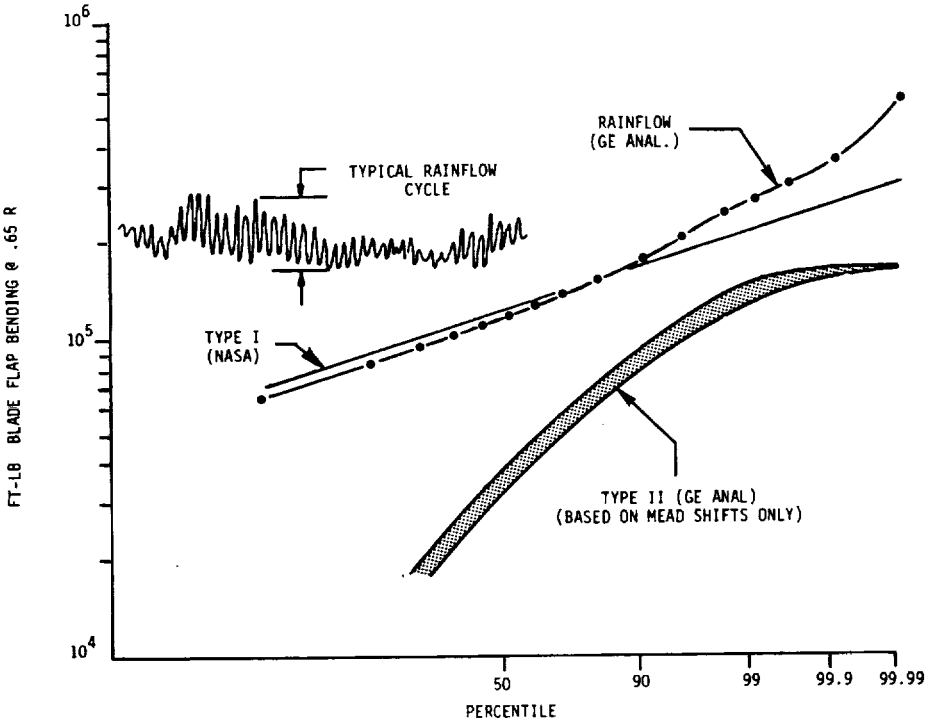

Figure 31. Rainflow Analysis of MOD-2 Test Data. Measurements Taken 3/11/82.